

2010

Full Numerical Simulation of an Object Oriented Program for Hermetic Reciprocating Compressors: Numerical Verification and Experimental Validation.

Oriol Lehmkuhl
Termo Fluids

Rashmin Damle
CTTC - UPC

Joaquim Rigola
CTTC - UPC

Joan López
CTTC - UPC

Follow this and additional works at: <http://docs.lib.purdue.edu/icec>

Lehmkuhl, Oriol; Damle, Rashmin; Rigola, Joaquim; and López, Joan, "Full Numerical Simulation of an Object Oriented Program for Hermetic Reciprocating Compressors: Numerical Verification and Experimental Validation." (2010). *International Compressor Engineering Conference*. Paper 2013.
<http://docs.lib.purdue.edu/icec/2013>

This document has been made available through Purdue e-Pubs, a service of the Purdue University Libraries. Please contact epubs@purdue.edu for additional information.

Complete proceedings may be acquired in print and on CD-ROM directly from the Ray W. Herrick Laboratories at <https://engineering.purdue.edu/Herrick/Events/orderlit.html>

Full Numerical Simulation of an Object Oriented Program for Hermetic Reciprocating Compressors: Numerical Verification and Experimental Validation.

Oriol LEHMKUHL^{1,2}, Rashmin DAMLE¹, Joaquim RIGOLA^{1*}, Joan LÓPEZ¹

¹Centre Tecnològic de Transferència de Calor (CTTC),
Universitat Politècnica de Catalunya (UPC),
Colon 11, 08222 Terrassa (Barcelona), Spain
Tel. +34-93-739.81.92; FAX: +34-93-739.89.20
E-mail: cttc@cttc.upc.edu <http://www.cttc.upc.edu>

²TermoFluids, S.L.
Magí Colet 8, 08204 Sabadell (Barcelona), Spain
E-mail: termofluids@termofluids.com

ABSTRACT

An object oriented approach of the numerical simulation model for the thermal and fluid dynamic behavior of hermetic reciprocating compressors was previously presented (Damle, et al., 2008), describing the fluid flow resolution and its numerical verification, based on an updated version of the conservation equations resolution (continuity, momentum and energy) along the whole compressor domain in a sequential way (Pérez-Segarra, et al. 2003). In the present paper, not only a numerical verification is shown, but also an experimental validation is detailed, including to the object oriented code the heat transfer resolution between solid parts and its coupling with the fluid flow through compressor elements, in addition to kinematic and dynamic analysis of crankshaft vs. connecting rod mechanism. The present full object oriented numerical simulation program, together with a brief numerical verification is here presented, while a detailed experimental validation for different compressor capacities, fluid refrigerants and working fluids is also shown in order to assure the numerical results obtained and the possibilities offered by the new program.

1. INTRODUCTION

Numerical simulations are often sought to predict the thermal and fluid dynamic behavior of reciprocating compressors which consists of complex transient heat transfer, compressible flow, three-dimensional, turbulent and pulsatory processes. Different compressor simulation models are found in the literature. Models by Pérez-Segarra, et al. (1994, 2003) and Rigola, et al. (2003, 2004) which are based on full integration of the one-dimensional and transient governing equations (continuity, momentum and energy) through all the compressor domain in a sequential way with experimental validation have been published in detail. Longo and Gasparella (2003) did an unsteady state analysis of the compressor cycle with a one dimensional valve model. Model by Duprez, et al. (2007) is based on thermodynamic analysis of the compressor while Elhaj, et al. (2008) presented the numerical simulation of a two-stage reciprocating compressor for predictive condition monitoring. These global simulation models need closure relations such as pressure drop coefficients across tubes and singularities, convective heat transfer coefficients, fluid flow through valves, leakage parameters, etc.

The work presented here applies an unstructured object-oriented modular methodology for the numerical simulation of the elements forming the compressor domain to predict the thermal and fluid dynamic behavior (temperature, pressure, mass flow rates, power consumption, etc.) of the compressor, together with heat transfer analysis between solid zones and fluid flow domain, in addition with mechanical analysis of crankshaft connecting rod mechanism. Each element (an object from C++ point of view) may have different levels of simulation with different models. Other models like CFD&HT resolution, parametric correlation based on experimental data, numerical results, etc. for a given element can be easily incorporated in the code. Modularity of the compressor domain adds flexibility in handling new compressor circuitry (e.g. having parallel lines, more than one compression chamber in series or parallel, multiple inlets/outlets, etc.). Moreover, an object oriented modular code adapts to new configurations easily by adding or removing elements and offers code reusability. Description of the modular methodology, mathematical formulation, numerical resolution, test verification and experimental comparison are presented in the following sections.

2. MODULAR COMPRESSION DOMAIN

The compressor domain is divided into separate elements (objects from C++ point of view). Figure 1 shows the most simplified compressor domain. The objects developed here are: i) *Fixed Value*: a boundary condition object specifying temperature and pressure values; ii) *Tube*: cylindrical element having small diameter in comparison with the length; iii) *Valve Orifice*: cross-section allowing mass flow through it depending on the valve parameters and pressure difference across it; iv) *Chamber*: sufficiently large and fixed volume of gas with multiple inlet and/or outlet tubes connections; v) *Compression chamber*: specific chamber with variable volume connected to valve orifices. These basic objects are linked together to form a given compressor circuit. Each object is capable of solving itself for given boundary conditions received from its neighbors.

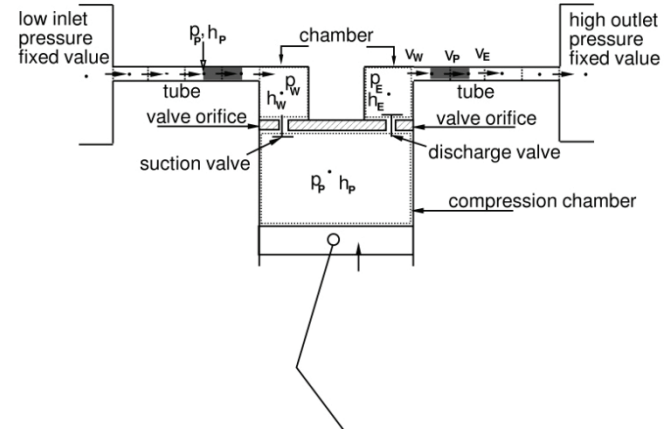


Figure 1: Simplest combination of compressor domain.

3. CRANKSHAFT - CONNECTION ROD MECHANISM

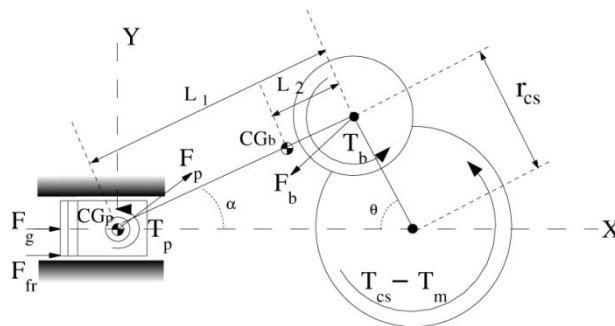


Figure 2: Mechanism forces scheme.

The kinematic equations are evaluated according to Pérez-Segarra et al. (2003), based on the compressor drive mechanism geometry, and the force/torque balances on the piston and crankshaft-connecting rod assembly (see Figure 2). The numerical resolution depends on the chamber gas pressure from fluid flow balance and motor torque from experimental data. The resulting algebraic system of equations shown below allows evaluating instantaneous crank angle acceleration $\ddot{\theta}$, piston connecting rod \vec{F}_p and the crank shaft connecting rod forces \vec{F}_b . This gives in turn the instantaneous angular velocity and the crank angle position. The chamber volume is then calculated based on the crank angle position.

Equations (1) to (5) show force and momentum of the free solid balances on the crankshaft connecting rod mechanical system of Figure 2.

$$F_g + F_{fr} - F_{px} = (m_p + m_{wp})\ddot{x}_{CG_p} \quad (1)$$

$$F_{px} - F_{bx} = m_b\ddot{x}_{CG_b} \quad (2)$$

$$F_{py} - F_{by} = m_b\ddot{y}_{CG_b} \quad (3)$$

$$F_{px} \left(1 - \frac{L_2}{L_1}\right) r_{cs} \sin \theta - F_{py} \left(1 - \frac{L_2}{L_1}\right) \sqrt{L^2 - r_{cs}^2 \sin^2 \theta} + F_{bx} \frac{L_2}{L_1} r_{cs} \sin \theta - F_{by} \frac{L_2}{L_1} \sqrt{L^2 - r_{cs}^2 \sin^2 \theta} + T_p - T_b = I_b \ddot{\alpha} \quad (4)$$

$$-F_{bx} r_{cs} \sin \theta - F_{by} r_{cs} \cos \theta - T_m + T_{cs} + T_b = -I_{cs} \ddot{\theta} \quad (5)$$

The resulting algebraic system of equations is solved using a direct LU method. Instantaneous angular velocity $\dot{\theta}$, and crank angle position θ are obtained from instantaneous angular acceleration $\ddot{\theta}$ using Adam-Hamilton implicit second order fully implicit method. Based on crank angle position, piston position x_{CG_p} and compression chamber volume V can be finally evaluated. An iterative loop is required due to the coupling between chamber pressure and its volume.

4. FLUID FLOW DISCRETIZED EQUATIONS

The numerical model is based on the division of the compressor domain into separate elements where the gas is flowing and these in turn are divided into a given number of control volumes depending on the type of the element. For example, the gas in a chamber or a compressor chamber is represented with only one CV and the gas through a tube is divided into an arbitrary number of CVs. For each CV a grid node is assigned at its centre (see Figure 1) where pressure, enthalpy and density values are evaluated. A staggered arrangement, also shown in Figure 1 by the shaded area, is employed for evaluating velocities at the faces of the same main CVs. The general governing equations of continuity, momentum and energy, over any of the element CVs described above, are written in terms of the local averaged fluid variables neglecting body forces, axial shear stresses and axial heat conduction. The semi-discretized form of the continuity, momentum and energy equations is given by equations 6, 7 and 8 respectively. Density is calculated from the state equation $\rho = f(p, h)$.

$$\frac{\partial m_p}{\partial t} + \sum \dot{m}_k^s = 0 \quad (6)$$

$$\frac{\partial m_p^s \bar{v}_p^s}{\partial t} + \sum \dot{m}_k^s v_{k^s} = F_s \quad (7)$$

$$\frac{\partial m_p (\bar{h}_p + \bar{e}_{cp})}{\partial t} + \sum \dot{m}_k^s (h_k + e_{ck}) = V_p \frac{\partial \bar{p}_p}{\partial t} + \dot{Q}_{wall} \quad (8)$$

4.1 Fixed value object

A fixed value object serves as a boundary condition of the compressor domain. Pressure and temperature values can be set for a fixed value object. It gives these values to the tubes connected to it. For example, it would serve as a reservoir shown in Figure 1 with set temperature and pressure values.

4.2 Numerical resolution of tube elements

The tube continuity equation is resolved over the main control volume as in Figure 1 with first order backward difference scheme for the unsteady term. A pressure correction equation is obtained from equation (6), according to the SIMPLEC method (Patankar, 1980), by estimating velocity v , density ρ and pressure p as the sum of guessed (ρ^* , v^* and p^*) and the correction values (ρ' , v' and p') respectively to verify the continuity equation. The energy equation is obtained by expanding equation (8) over a centered CV. The general momentum equation is written over a staggered mesh shown by the shaded areas in Figure 1. The semi-discretized form of the same considering the local shear stress in terms of friction factor is as follows:

$$\frac{\partial m_p^s \bar{v}_p^s}{\partial t} + \sum \dot{m}_{e^s} v_{e^s} - \sum \dot{m}_{w^s} v_{w^s} = (p_p - p_E) S - \frac{f}{4} \frac{|\dot{m}_p^s| v_p^s}{2S} A_p \quad (9)$$

The values of inlet temperature and pressure and outlet pressure are given as boundary conditions. The tube object can be connected with: i) a fixed value element; ii) another tube or iii) a chamber. When a tube is connected with a fixed value element the boundary condition for the tube momentum equation (7) is put assuming complete recovery/conversion of pressure in to velocity at eh boundary as:

$$(p_\infty - p_b) = \pm \rho v^2 / 2 = \pm |\dot{m}_b^s| v_b^s / 2S \quad (10)$$

where, p_b is the boundary pressure related to the fixed value pressure p_∞ and \dot{m}_b^s is the mass flow rate at the boundary. Also, anechoic boundary condition (i.e., the tube is infinite for the exit waves to be dissipated) can be applied. This is done as:

$$(p_\infty - p_b) = \rho c (v - \bar{v}) = c |\dot{m}_b^s| (1 - \bar{v}/v_b^s) / S \quad (11)$$

where, c is the velocity of sound, \bar{v} is the mean velocity at the exit averaged over time.

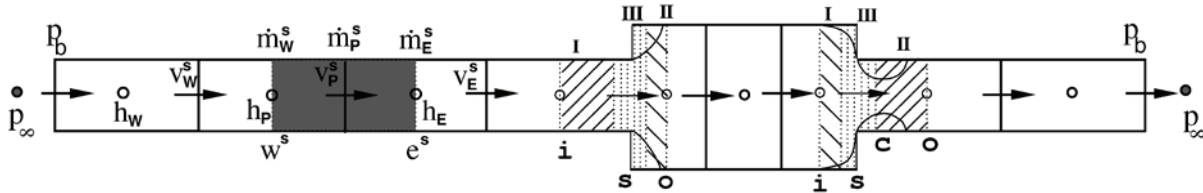


Figure 3: General discretization over different tubes scheme including contraction and expansion processes.

In case of sudden expansion or contraction as Figure 3 shown, or when tubes are connected to other tubes or chambers, the following momentum equation (12) is used to relate the pressures across expansion/contraction (Morse, 1953).

$$(p_b^I - p_b^{II})S^S = \frac{|\dot{m}_p^s| v_p^s}{2} \left\{ \left(\frac{(S^S)^2}{(S^{II})^2} - \frac{(S^S)^2}{(S^I)^2} \right) + \left(\frac{S^S}{S^o} - \frac{1}{c_c} \right)^2 \right\} + l \frac{\partial \dot{m}}{\partial t} \quad (12)$$

The length l , in the transient term of equation (12) is composed by the actual length of the constriction plus a correction term to allow for the extra fluid speeding up and slowing down at the two ends (Pérez-Segarra, et al. 2003). The contract coefficient $c_c = f(S^o/S^s)$ is a function of area ratios at the respective cross-sections.

The momentum equation across the expansion/contraction can be written in terms of mass flow rate in a general form by summing the momentum equations for zone I, II and III as:

$$\dot{m}_p = \frac{N(p_i - p_o) + H + (l\dot{m}_p^o/\Delta t)}{M} \quad (13)$$

where, N is the cross-sectional area S^s , \dot{m}_p^o is the mass flow rate at previous instant while H and M are the transient, convective and shear stress terms for zone I, II and III coming from the momentum equation.

4.3 Valve orifice dynamics

A momentum equation similar to the expansion/contraction, under the assumption of ideal gas evolution in a subsonic expansion and isentropic process Browler, et al. (1993), extended to compressible flow by taking into account the effective flow area $(KS)_s$ and maintaining the transient term l written as:

$$(p_u - p_d)(KS)_s = \frac{|\dot{m}| v_s}{2} \frac{\gamma - 1}{\gamma} \frac{1 - p_d/p_u}{\Pi^{1/\gamma} - \Pi} + l \frac{\partial \dot{m}}{\partial t} \quad (14)$$

The subscripts u and d refer to upstream and downstream conditions respectively. The parameter Π depends on flow conditions. In supersonic flow conditions $\Pi = \Pi_c = \left(\frac{2}{\gamma + 1} \right)^{\frac{\gamma}{\gamma - 1}}$, while under subsonic conditions $\Pi = \frac{p_d}{p_u} > \Pi_c$. Thus,

$\Pi = \max\left(\frac{p_d}{p_u}, \Pi_c\right)$ is valid for both cases.

The above equation can also be written in a form similar to that for expansion/contraction as equation (13) considering, $N = (KS)_s$, $H = 0$; $M = (l/\Delta t) + (|\dot{m}|^2 \Pi^{1/\gamma}) / (2\rho(KS)_s \gamma^2)$.

The valve position is calculated assuming a spring loaded ring valve governed by one degree of freedom. The valve displacement z depends on the effective area $(KS)_s$ which in turn depends on z . Therefore, during the simulation, the valve displacement z is calculated iteratively as a function of the pressures on either side of the valve. The effective area $(KS)_s$ is then calculated from z and the mass flux thus obtained from equation (13) is set as output for its neighbors.

4.4 Chamber and Compression Chamber

The chamber element has only one CV and can have multiple tube connections (inlets/outlets) or valve orifice elements. In this case, the continuity equation over the chamber CV is rearranged as a pressure correction equation for obtaining a pressure correction as a function of the pressure values of the neighbor elements at the CVs adjacent to the chamber. Mass flow rates are evaluated from the momentum equations applied over a staggered mesh for all the neighbor elements connected at the face of the chamber CV. An iterative algorithm is applied within the chamber at each iteration until convergence is reached in order to obtain the chamber pressure and

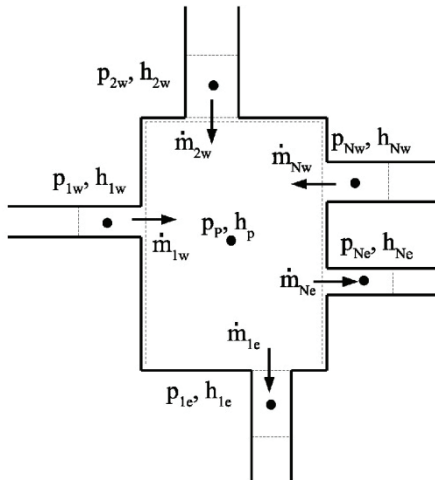


Figure 4a: Chamber discretization scheme.

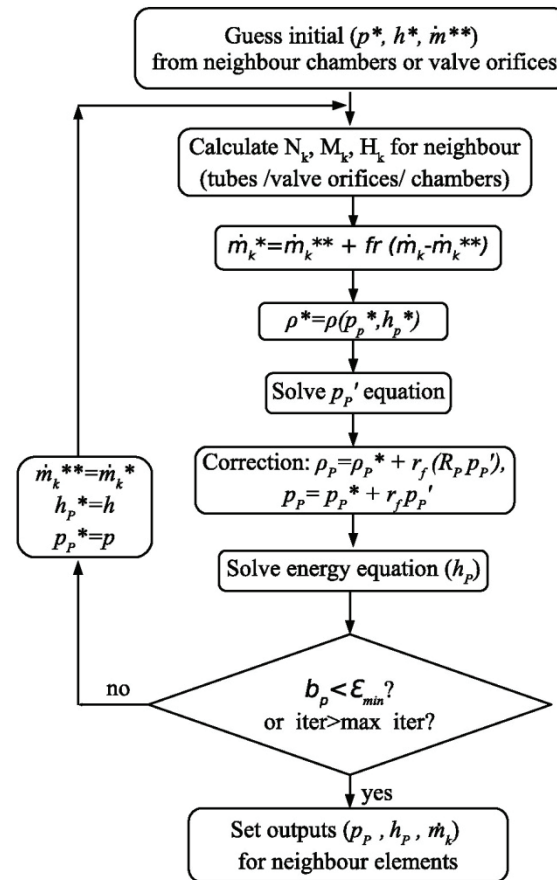


Figure 4b: Chamber resolution algorithm.

enthalpy as a function of the pressures of the neighbor elements around the chamber CV. Figure 4a depicts the CV connections around a chamber element and the information needed from the neighbors, while Figure 4b details the compressor chamber resolution for every iteration of a given time step.

The mass flow rate at each connection (tube or valve orifice) is written as

$$\dot{m}_k = \frac{N_k(p_p - p_k) + H_k + (I_k \dot{m}_k^o / \Delta t)}{M_k} \quad (15)$$

where, variables take different values for valve orifices and tubes. The subscript k indicates the different elements connected to the compression chamber/chamber. From this equation a mass correction is sought as: $\dot{m}'_k = d_k(p'_p - p'_k)$ where $d_k = N_k/M_k$ and put in the continuity equation (6) to obtain an equation for pressure correction p' for compression chamber/chamber. Here, flow entering the chamber is considered positive (west) and leaving as negative (east). The compression chamber/chamber gets pressure from the tubes and valve orifices as data. Thus, $p'_{kE} = 0$ and $p'_{kW} = 0$. The compression chamber/chamber resolution consists of the following steps, based on Figure 4b for every iteration: i) From guess initial values based on mass flow rate coming from tubes and valve orifices, density is calculated as $\rho_p^* = \rho(p_p^*, h_p^*)$; ii) Parameters N_k , H_k and M_k are evaluated from respective neighbours and \dot{m}_k^* is evaluated; iii) Correction pressure p'_p over chamber is obtained from correction pressure equation; iv) Pressure and density over chamber is then updated; v) Enthalpy over chamber is obtained from energy equation; and finally vi) Iterative loop is carried out until convergence of pressure, enthalpy, density over chamber and mass flow rate across each one of inlet/outlet sections is reached.

5. GLOBAL RESOLUTION ALGORITHM

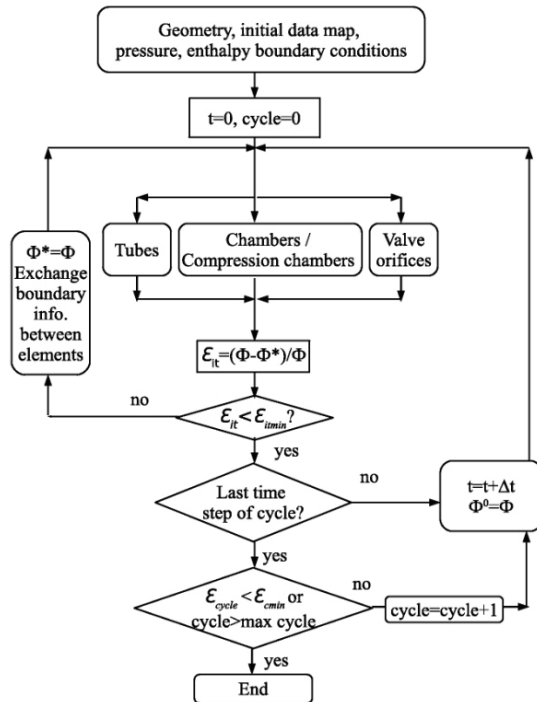


Figure 5: Compressor global resolution algorithm.

The compressor domain formed by connecting the different elements (e.g. fixed value objects, tubes, chambers, valves and compression chambers), is simulated in an iterative manner. The global algorithm is shown in Figure 5.

The fixed value objects with set temperature and pressure values act as the boundary conditions of the compressor domain. The program control goes through all the elements once every iteration. An iteration for the given element at each time step consists of the following steps:

- Get inputs (p, h, \dot{m}, \dots) from the neighbour elements.
- Solve the governing equations of the element (direct TDMA for tubes or iterative loop for chamber/compression chamber).
- Set outputs (p, h, \dot{m}, \dots) for the neighbour elements.

The iterations are continued by updating the variables after each iteration until the convergence criteria for each time step is reached. Transient calculation then continues until cyclic steady state is reached.

6. RESULTS

Several numerical test cases (Damle, et al., 2008) have been carried out in order to assure the quality of the numerical solution by means of a critical analysis of the different numerical source of errors: programming errors, convergence errors and discretization errors. The numerical cases have been performed not only to ensure asymptotic solution with mesh refinements and convergence criteria, but also achieving physically realistic results with the accomplishment of mass and energy conservation. In the present paper, 2 numerical verification tests are presented considering the case of a chamber connected with 5 tubes like Figure 4a, together with the case of a compression chamber like Figure 1, without reed valve (i.e., valves kept always open) with equal inlet and outlet pressure during cyclic conditions. After numerical verification several numerical cases are experimentally validated against different compressor capacities, fluid refrigerants and working conditions.

6.1 Numerical verifications

Table 1 shows the numerical results of a chamber with multiple tubes of different diameters across a pressure difference (3 tubes with an inlet pressure of 55 bar and non-dimensional diameter d^* equal to 1, 0.2 and 0.6; and 2 tubes with an outlet pressure of 50 bar and d^* equal to 0.4 and 0.8). The whole mass flow rate through inlet tubes is compared against outlet tubes, together with the error in mass balance.

Table 1: Chamber with multiple inlet/outlet tubes accuracy numerical results evolution.

\mathcal{E}_{steady}	10^{-4}	10^{-5}	10^{-6}	10^{-7}	10^{-7}
$\sum \dot{m}_{in}$ (kg/s)	0.5230	0.5234	0.523491	0.5234946	0.5234950
$\sum \dot{m}_{out}$ (kg/s)	0.5238	0.5235	0.523498	0.5234954	0.5234951
m_{error} (kg/s)	$7.63 \cdot 10^{-4}$	$7.23 \cdot 10^{-5}$	$7.26 \cdot 10^{-6}$	$7.27 \cdot 10^{-7}$	$7.28 \cdot 10^{-8}$
$T_{chamber}$ (°C)	309.29	309.42	309.43	309.44	309.44

Numerical results show how absolute error in mass balance diminishes with the accuracy for steady state, together with chamber temperature assures asymptotic solution.

Table 2 shows the numerical results of a compressor domain as Figure 1, without reed valve, with equal inlet and outlet pressures in order to check cyclic asymptotic conditions. The whole mass flow rate though inlet tubes is compared against outlet tubes, together with the error in mass balance.

Table 2: Numerical verification compressor domain cyclic results.

$\varepsilon_{\Delta t} / \varepsilon_{cyclic}$	10^{-2}	10^{-3}	10^{-4}	10^{-5}	10^{-6}
\dot{m} (kg/h)	29.679	29.61659	29.61659	29.61650	29.61650
T_{out} (°C)	101.762	101.7707	101.7708	101.7708	101.7708
W (J)	10.0259	10.01047	10.01047	10.01047	10.01047

Numerical results show how absolute error in mass balance diminishes with the accuracy for steady state, together with chamber temperature assures asymptotic solution.

6.2 Experimental validation

Once the object oriented code is numerically verified, an experimental validation takes places. Table 3 shows the numerical results compared against experimental data of Rigola et al. (2003)(2005) for different compressor configurations working with R134a and R600a for compressor capacities of 8cm³ and 16cm³.

Table 3: Experimental validation of numerical simulation tool.

T_{evap} (°C)	Pressure ratio	Numerical			Experimental		
		\dot{m} (kg/h)	\dot{W}_e (W)	T_{out} (°C)	\dot{m} (kg/h)	T_{out} (°C)	\dot{W}_e (W)
7.2 (R134a)	4.03	18.82	343.3	88.5	17.42	310.7	83.8
0.0 (R134a)	5.14	14.11	300.6	89.0	13.02	273.0	83.7
-10.0 (R600a)	7.7	5.35	256.1	93.5	5.15	242.0	100.5
-23.3 (R600a)	12.83	2.70	171.2	92.5	2.64	169.0	100.5

Relative differences between numerical results and experimental data on mass flow rate, power consumption and outlet fluid flow compressor temperature are lower than 10% in all studied cases, which is reasonably accepted.

7. CONCLUSIONS

Modular and object oriented methodology, mathematical formulation and numerical resolution of the components forming the compressor domain together with their integration have been presented. A pressure correction algorithm is presented not only for the thermal and fluid dynamic analysis of the fluid inside tubes, but also for the chambers and compression chambers. Test cases have been carried out for the verification of the code. The code shows a consistent behavior and the numerical results are physically realistic. The numerical results presented show reasonably good agreement against the experimental data of different household and commercial hermetic compressors. Different refrigerants like R134a, R600a with different configurations and working conditions have been successfully validated. The new code developed offers flexibility in handling complex compressor circuitry and quick adaptability to new arrangements by addition or removal of the required elements.

NOMENCLATURE

A_p	perimeter area (m ²)	p	pressure
CG	centre of mass	p'	pressure correction
CV	control volume	\dot{Q}	heat rate (W)
c_c	contract coefficient	r_{cs}	crank shaft radius (m)
e_c	kinetic energy (J/kg)	S	area(m ²)
F	force (N)	S^I, S^{II}	expansion/contraction cross section (m ²)
h	enthalpy (J/kg)	t	time(sec)
H, N, M	terms from momentum equation	T	torque (Nm)
l	constriction length(m)	v	velocity(m/s)
L	connecting rod length (m)	V	Volume(m ³)
m	mass(kg)	\dot{W}_e	power consumption (W)
\dot{m}	mass flow rate(kg/s)	Y^e	compressibility factor
<i>Greek symbols</i>			
ϕ	generic variable (p, h, v)	ρ	density(kg/m ³)
ε	precision demanded	ρ'	density correction
γ	ratio of specific heats of a gas	α	relaxation factor for p'
θ	crank angle	Π	pressure ratio
<i>Superscripts</i>			
*	guess value	o	value at previous time step
–	overbar integral mass averages over CV	\sim	tilde integral volume average over CV
<i>Subscripts</i>			
P	central point or CV under consideration	W	point or CV to left(west) of P
E	point or CV to right(east) of P	k	connection index to the chamber
w	control volume face between W and P	e	control volume face between P and E
g	gas	fr	friction
cs	crank shaft	m	motor
wp	wrist pin	p	piston
b	connecting rod		

REFERENCES

- Browler, W.B., Eisler, Jr.E., Gonenc, E.J., Plati, C., Stagnitti, J., 1993, On the compressible flow through an orifice, J. Fluid Engineering, 115, p. 660-664.
- Damle, R., Rigola, J., Pérez-Segarra, C.D., Oliva, A., 2008, An Object Oriented Program for the Numerical Simulation of Hermetic Reciprocating Compressor Behaviour, International Compressor Engineering Conference, Purdue University, West Lafayette, Indiana, USA, C1402.
- Duprez, M., Dumont, E., Frre, M., 2007, Modelling of reciprocating and scroll compressors, International Journal of Refrigeration, 30,(5), pp.873-886.
- Elhaj, M., Gu, F., Ball, A.D., Albarbar, A., Al-Qattan, M., Naid, A., 2008, Numerical simulation and experimental study of a two-stage reciprocating compressor for condition monitoring, Mechanical Systems and Signal Processing, 22(2), pp.374-389.
- Longo, G.A., Gasparella, A., 2003, Unsteady state analysis of the compression cycle of a hermetic reciprocating compressor, International Journal of Refrigeration, 26:(6), pp.681-689.
- Morse, P.M., Feshbach, H., 1953, Methods of Theoretical Physics, part 2, McGraw-Hill Book Company.
- Patankar, S.V., 1980, Numerical Heat Transfer, Hemisphere publishing corporation.
- Pérez-Segarra, C.D., Escanes, F., Oliva, A., 1994, Numerical Study of the Thermal and Fluid-Dynamic Behaviour of Reciprocating Compressors, International Compressor Engineering Conference, Purdue University, West Lafayette, Indiana, USA, p. 145-150.
- Pérez-Segarra C.D., Rigola, J., Oliva, A., 2003, Modelling and numerical simulation of the thermal and fluid dynamic behaviour of hermetic reciprocating compressors. Part 1. Theoretical basis, Int J Heating, Ventilating, Air-Conditioning Refrigerating Res 9, p. 215-236.
- Rigola, J., Pérez-Segarra, C.D., Oliva, A., 2003, Modelling and numerical simulation of the thermal and fluid dynamic behaviour of hermetic reciprocating compressors. Part 2. Experimental investigation, Int J Heating, Ventilating, Air-Conditioning Refrigerating Res 9, p. 237-249.
- Rigola, J., Raush, G., Pérez-Segarra, C.D., Oliva, A., 2004, Detailed Experimental Validation of the Thermal and Fluid Dynamic Behaviour of Hermetic Reciprocating Compressors, Int J Heating, Ventilating, Air-Conditioning Refrigerating Res 10, p. 291-306.

ACKNOWLEDGEMENT

This work has been financially supported by the Ministerio de Ciencia e Innovación, Secretaría de Estado de Investigación, Spain (ref. ENE 2008-06667).